Eur. Phys. J. AP **6**, 61–70 (1999)

THE EUROPEAN PHYSICAL JOURNAL APPLIED PHYSICS

On the robust control of an induction machine: A complete design and realization

D.R. Chouiter, G. Clerc[a], P. Auriol, and J.M. Rétif

CEGELY[b], École Centrale de Lyon, B.P. 163, 69131 Écully Cedex, France

Received: 29 April 1998 / Revised: 19 October 1998 / Accepted: 23 December 1998

Abstract. Electrical traction of vehicle needs accurate control of torque and flux. DC machines are mainly used but they are expensive and need heavy maintenance. Since some years, the use of field oriented vector control induction machines allows to fulfill the same objectives with lower cost. Unfortunately, they may present a decrease of their performances and an instability when their parameters vary with the temperature or the magnetic state and in the presence of converter or measurement noises. Therefore it is necessary to design effective control laws, which are especially less sensitive to these perturbations and variations. In this work, we have undertaken the conception and the realization of a voltage vector flux control whose inputs have been uncoupled by compensating terms. The torque and the flux regulations are realized at two different levels: an internal regulation loop for stator currents, and an external one for flux and torque. In order to achieve robust stability and performance objectives, we have involved several new methods in the domain such as H_∞ control designed by genetic algorithms and reduced order extended Kalman filtering in the synchronous frame. Simulations will show the method efficiency and experimental results validate the control strategy.

PACS. 07.05.Dz Vacuum gauges – 84.50.+d Electric motors

Notations

R_r : rotor resistance/phase;
R_s : stator resistance/phase;
L_r : rotor inductance/phase;
L_s : stator inductance/phase;
L_m : magnetizing inductance;
T_r : rotor time constant $= L_\mathrm{r}/R_\mathrm{r}$;
T_s : stator time constant $= L_\mathrm{s}/R_\mathrm{s}$;
σ : $\sigma = 1 - L_\mathrm{m}^2/(L_\mathrm{s}L_\mathrm{r})$;
σ_r : $\sigma_\mathrm{r} = R_\mathrm{r}/L_\mathrm{r}$;
J : inertia;
f : friction coefficient;
p : number of pair of poles;
ω_s : stator current pulsation;
ω_m : mechanical pulsation;
ω_sl : rotor current pulsation $\omega_\mathrm{sl} = \omega_\mathrm{s} - \omega_\mathrm{m}$;
T_ech: sampling period;
T_e : electromagnetic torque;
T_l : load torque;
Ω : mechanical speed;
Φ_dr : rotor flux component on d axis;
Φ_qr : rotor flux component on q axis.

[a] e-mail: guy.clerc@trotek.ec-lyon.fr
[b] CNRS No. 5005

1 Introduction

Low cost and robust AC motors are now used in variable speed applications. In order to provide independent regulation of torque and flux with fast transient response, they are often controlled with a field oriented vector control strategy. But resistance and inductance changes with temperature or operating point decrease their dynamic performances. Furthermore electromagnetic and numeric noise can induce instability.

This paper presents a robust control strategy used with a voltage fed asynchronous motor, which decreases these drawbacks.

Indirect rotor field oriented vector drive strategy, state space decoupling and current controllers are implemented in a synchronous *d-q* reference frame. Thus, torque and flux are independently fixed by stator current references.

The torque and flux regulation is realized at two levels: an internal regulation loop for stator currents, and an external loop for the regulation of torque and flux.

Fixed order current controllers are obtained by a robust H_∞ synthesis researching an *a priori* compromise between performance and stability in function of noise in the process and parameter variations. Automatic design is provided by genetic algorithm.

The control of torque and flux is realized by the implementation of a Kalman filter giving an estimation of the rotor time-constant and flux.

During this work, we have developed methodologies and validate our results with simulations and real time implantation on an asynchronous motor bench.

2 Field oriented control of asynchronous machine

In order to design current controllers and flux estimators, it is necessary to perform the open loop model of the voltage-fed induction motor. It is represented in a *d-q* synchronous reference frame by the following equations:

$$\frac{\mathrm{d}X}{\mathrm{d}t} = AX + BU \tag{1}$$

with:

$$A = \begin{bmatrix} -\left(\frac{1}{T_\mathrm{s}\sigma} + \frac{1}{T_\mathrm{r}}\frac{1-\sigma}{\sigma}\right) & \omega_\mathrm{s} & \frac{1-\sigma}{\sigma}\frac{1}{L_\mathrm{m}T_\mathrm{r}} & \frac{1-\sigma}{\sigma}\frac{1}{L_\mathrm{m}}\omega_\mathrm{m} \\ -\omega_\mathrm{s} & -\left(\frac{1}{T_\mathrm{s}\sigma} + \frac{1}{T_\mathrm{r}}\frac{1-\sigma}{\sigma}\right) & -\frac{1-\sigma}{\sigma}\frac{1}{L_\mathrm{m}}\omega_\mathrm{m} & \frac{1-\sigma}{\sigma}\frac{1}{L_\mathrm{m}T_\mathrm{r}} \\ \frac{L_\mathrm{m}}{T_\mathrm{r}} & 0 & -\frac{1}{T_\mathrm{r}} & \omega_\mathrm{sl} \\ 0 & \frac{L_\mathrm{m}}{T_\mathrm{r}} & \omega_\mathrm{sl} & -\frac{1}{T_\mathrm{r}} \end{bmatrix}$$

$$B = \begin{bmatrix} \frac{1}{\sigma L_\mathrm{s}} & 0 \\ 0 & \frac{1}{\sigma L_\mathrm{s}} \\ 0 & 0 \\ 0 & 0 \end{bmatrix}, \quad X = \begin{bmatrix} i_\mathrm{ds} \\ i_\mathrm{qs} \\ \phi_\mathrm{dr} \\ \phi_\mathrm{qr} \end{bmatrix}, \quad U = \begin{bmatrix} v_\mathrm{ds} \\ v_\mathrm{qs} \end{bmatrix}.$$

The torque may be expressed as follows:

$$T_\mathrm{e} = \frac{pL_\mathrm{m}}{L_\mathrm{r}}(\phi_\mathrm{dr} i_\mathrm{qs} - \phi_\mathrm{qr} i_\mathrm{ds}). \tag{2}$$

Rotor field orientation, in a rotating synchronous reference frame realizes [1–5]: $\phi_\mathrm{qr} = 0$ and $\phi_\mathrm{dr} = \phi_\mathrm{r} = constant$.

According to equations (1, 2), one can write:

$$v_\mathrm{ds} = \sigma L_\mathrm{s}\frac{\mathrm{d}i_\mathrm{ds}}{\mathrm{d}t} + \left(R_\mathrm{s} + R_\mathrm{r}\frac{L_\mathrm{m}^2}{L_\mathrm{r}^2}\right) i_\mathrm{ds} - \omega_\mathrm{s}\sigma L_\mathrm{s} i_\mathrm{qs} - \frac{L_\mathrm{m}}{L_\mathrm{r}^2} R_\mathrm{r}\phi_\mathrm{r}^* \tag{3}$$

$$v_\mathrm{qs} = \sigma L_\mathrm{s}\frac{\mathrm{d}i_\mathrm{qs}}{\mathrm{d}t} + \left(R_\mathrm{s} + R_\mathrm{r}\frac{L_\mathrm{m}^2}{L_\mathrm{r}^2}\right) i_\mathrm{qs} + \omega_\mathrm{s}\sigma L_\mathrm{s} i_\mathrm{ds} + \frac{L_\mathrm{m}}{L_\mathrm{r}}\omega_\mathrm{m}\phi_\mathrm{r}^* \tag{4}$$

and

$$T_\mathrm{r}\frac{\mathrm{d}\phi_\mathrm{r}^*}{\mathrm{d}t} + \phi_\mathrm{r}^* = L_\mathrm{m} i_\mathrm{ds} \tag{5}$$

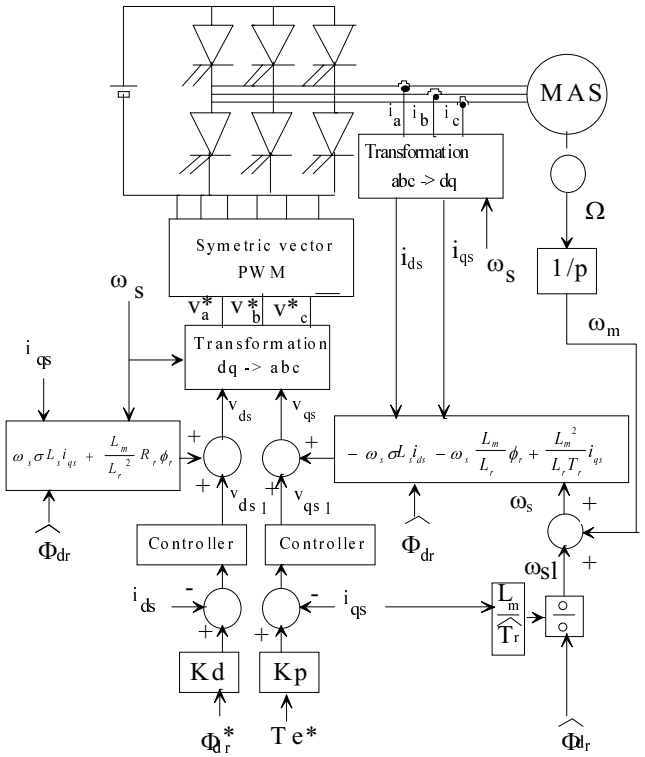

Fig. 1. Oriented field control drive of asynchronous machines.

$$\omega_\mathrm{sl} = \frac{L_\mathrm{m}}{\phi_\mathrm{r}^* T_\mathrm{r}} i_\mathrm{qs} \tag{6}$$

$$T_\mathrm{e} = \frac{pL_\mathrm{m}}{L_\mathrm{r}}\phi_\mathrm{r} i_\mathrm{qs} \tag{7}$$

where ϕ_r^* represents the rotor flux reference.

Equations (3, 4) involves mutual actions on *d-q* axes: a voltage applied on one axis induces current components on both axes. Flux and torque are no longer independently controlled by *d* and *q* inputs.

Thus, two new reference inputs v_ds1 and v_qs1 are introduced in order to uncouple this system (Fig. 1)

$$\begin{cases} v_\mathrm{ds1} = v_\mathrm{ds} + \mathrm{fem_d} \\ v_\mathrm{qs1} = v_\mathrm{qs} + \mathrm{fem_q} \end{cases}$$

with

$$\begin{cases} \mathrm{fem_d} = \omega_\mathrm{s}\sigma L_\mathrm{s} i_\mathrm{qs} + \dfrac{L_\mathrm{m}}{L_\mathrm{r}^2} R_\mathrm{r}\phi_\mathrm{r}^*, & (8) \\ \mathrm{fem_q} = -\omega_\mathrm{s}\sigma L_\mathrm{s} i_\mathrm{ds} - \omega_\mathrm{s}\dfrac{L_\mathrm{m}}{L_\mathrm{r}}\phi_\mathrm{r}^* + \dfrac{L_\mathrm{m}^2}{L_\mathrm{r}T_\mathrm{r}} i_\mathrm{qs}. & (9) \end{cases}$$

Finally, this control provides a diagonal transfer matrix:

$$\begin{bmatrix} i_\mathrm{ds} \\ i_\mathrm{qs} \end{bmatrix} = M \begin{bmatrix} v_\mathrm{ds1} \\ v_\mathrm{qs1} \end{bmatrix}$$

with:

$$M = \begin{bmatrix} \frac{L_\mathrm{r}T_\mathrm{r}}{R_\mathrm{s}L_\mathrm{r}T_\mathrm{r} + L_\mathrm{m}^2 + \sigma L_\mathrm{s}L_\mathrm{r}T_\mathrm{r}s} & 0 \\ 0 & \frac{L_\mathrm{r}T_\mathrm{r}}{R_\mathrm{s}L_\mathrm{r}T_\mathrm{r} + L_\mathrm{m}^2 + \sigma L_\mathrm{s}L_\mathrm{r}T_\mathrm{r}s} \end{bmatrix}. \tag{10}$$

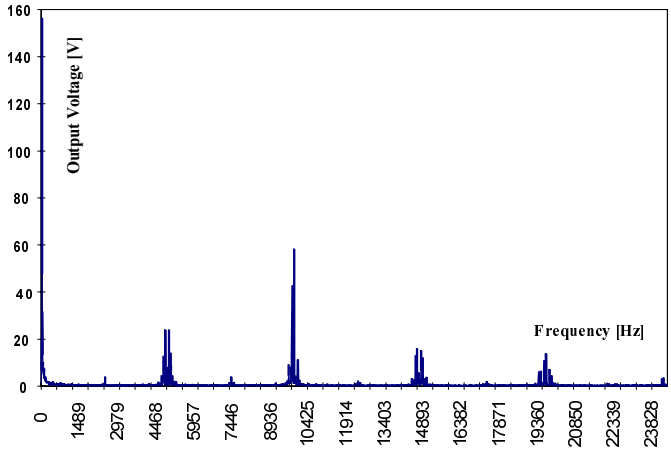

Fig. 2. PWM voltage spectrum with a 10 kHz low-pass filter.

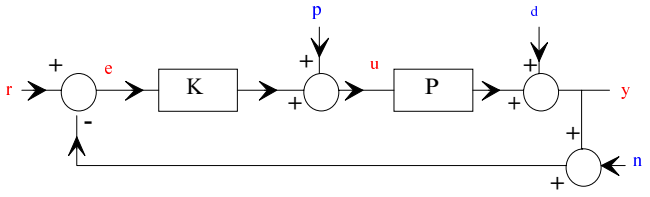

Fig. 3. Typical closed loop.

Finally, the rotor flux indirect oriented field scheme is representing in Figure 1. Near the nominal operating point, it provides independent control of torque and flux.

Let us note $K_\mathrm{d} = 1/L_\mathrm{m}$ and $K_\mathrm{p} = L_\mathrm{r}/pL_\mathrm{m}\Phi^*_\mathrm{dr}$.

Therefore resistances drift with temperature and noises injected by the Pulse Width Modulation (PWM) or induced by delays involve decrease of performance of the current loop system [12]. We will see later that H_∞ synthesis takes into account these problems.

Furthermore, equation (6) shows that the slip frequency depends on the rotor time constant T_r. Thus a variation on this resistance induces a lack of orientation. Extended reduced order Kalman filter provides an adaptive scheme.

3 Noise and parameter variation

3.1 Noise in the process

A three-phase vector symmetric pulse width modulation drives the inverter. Thus, the mean values of AC motor supply voltages during the sampling period (defined by a two kHz clock) equal to the desired control law references.

But, this PWM inject high frequency harmonics in the input of the process. Figure 2 shows the output voltage spectrum for a sinusoidal 50 Hz reference. In addition to that, speed sensor brings noises in the feedback loop.

All of theses noises can be represented by the signals n, d and p (Fig. 3), where n is the sensor noise, d the perturbations on the output current, and p the noise on the input voltage.

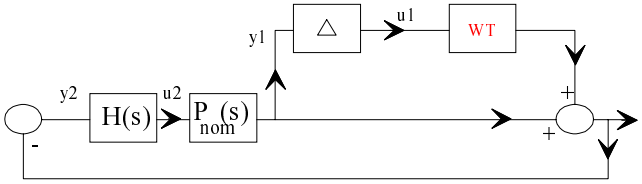

Fig. 4. Stability.

$P_\mathrm{nom}(s)$ is the transfer function of the field oriented decoupled machine nominal model and $H(s)$ is the transfer function of the controller.

3.2 Model

variation The machine parameters may vary during the operation. Rotor resistance changes with temperature and skin effect. Inductance vary with saturation.

These variations can be considered as unstructured multiplicative model uncertainties.

From the definition proposed by many authors, unstructured uncertainties can cover a large panel of differences between models and real physical systems such as unmodeled dynamics and some non linearities [8,9]. The synthesis of the H_∞ controller is achieved considering the variation of the linear plant P_nom

$$P_\mathrm{nom}(s) = \frac{L_\mathrm{r}T_\mathrm{r}}{R_\mathrm{s}L_\mathrm{r}T_\mathrm{r} + L_\mathrm{m}^2 + \sigma L_\mathrm{s}L_\mathrm{r}T_\mathrm{r}s}\cdot \qquad (11)$$

Let Δ_m denote the perturbation representing parameter variation in the nominal plant. The perturbed plant P is written as:

$$P(s) = P_\mathrm{nom}(s)(1 + \Delta_\mathrm{m}(s)) \qquad (12)$$

with:

$$\Delta_\mathrm{m}(s) = \Delta(s)W_\mathrm{T}(s). \qquad (13)$$

$W_\mathrm{T}(s)$ is a fixed stable transfer function called multiplicative perturbation weighting function. $\Delta(s)$ is a variable stable transfer function satisfying $\|\Delta(\mathrm{j}w)\|_\infty < 1$ (Fig. 4). Thus, $|W_\mathrm{T}(\mathrm{j}\omega)|$ provides the uncertainty profile.

4 Current inner control loop designed with H_∞ synthesis

Controllers must keep stability and dynamic performances of the current loop in spite of parameter variation and noises. The algorithm has to be implemented in a low cost micro-controller. Thus, the parameters of the current correctors must be kept constant (no adaptive scheme in the inner loop) and these regulators must have a low order structure. So H_∞ synthesis has been used to design them and to realize the best compromise between stability and performance robustness. First, H_∞ theory will be summarized. Then application will be presented.

4.1 Sensitivity and complementary sensitivity functions

In order to quantify stability and performance, we must define the sensitivity function S and the complementary sensitivity function T:

$$S_{\mathrm{nom}}(s) = (1 + L_{\mathrm{nom}}(s))^{-1} = \frac{y(s)}{d(s)} \tag{14}$$

$$T_{\mathrm{nom}}(s) = L_{\mathrm{nom}}(s)(1 + L_{\mathrm{nom}}(s))^{-1} = \frac{y(s)}{r(s)} \tag{15}$$

$$L_{\mathrm{nom}}(s) = P_{\mathrm{nom}}(s)H(s) \tag{16}$$

where $L_{\mathrm{nom}}(s)$ is the nominal open-loop transfer function and y and r represent respectively the output and the reference currents.

$S_{\mathrm{nom}}(s)$ determines the disturbance attenuation since S_{nom} is the closed-loop transfer function from disturbance d to plant output i_{ds}.

A disturbance attenuation specification can be written as:

$$|S_{\mathrm{nom}}(\mathrm{j}\omega)| < \frac{1}{|W_{\mathrm{S}}(\mathrm{j}\omega)|} \tag{17}$$

where $|W_{\mathrm{S}}^{-1}(\mathrm{j}\omega)|$ is the desired disturbance attenuation factor perturbation according to the frequency.

$T_{\mathrm{nom}}(s)$ is used to measure the stability margins in the presence of multiplicative plant perturbations (Δ_{m}):

$$| T_{\mathrm{nom}}(\mathrm{j}\omega) | < \frac{1}{| W_{\mathrm{T}}(\mathrm{j}\omega) |} \tag{18}$$

where $|W_{\mathrm{T}}(\mathrm{j}\omega)|$ defines the largest multiplicative plant perturbation according to the frequency. In order to satisfy $S_{\mathrm{nom}}(s) + T_{\mathrm{nom}}(s) = 1$, the following condition must be achieved:

$$\left|\frac{1}{W_{\mathrm{S}}(\mathrm{j}\omega)}\right| + \left|\frac{1}{W_{\mathrm{T}}(\mathrm{j}\omega)}\right| > 1. \tag{19}$$

From considerations above, one can see that the choice of the weighting functions W_{S} and W_{T} is of a great importance to guarantee robust stability and nominal performance of the closed-loop system.

The infinity norm of a plant $H(s)$ is defined as follows:

$$\|H(\mathrm{j}\omega)\|_\infty := \sup_\omega |H(\mathrm{j}\omega)|. \tag{20}$$

In terms of infinity norm, nominal performance and robust stability of the closed-loop system are achieved if the two following relations are respectively verified:

$$\left\|W_{\mathrm{S}}S_{\mathrm{nom}}\right\| < 1 \quad \text{and} \quad \left\|W_{\mathrm{T}}T_{\mathrm{nom}}\right\| < 1. \tag{21}$$

4.2 Weighting functions specification

Weighting functions are chosen according to the expected model uncertainty and performance. Their shapes depend on the PWM noise spectrum, the cut-off frequencies. They are not unique.

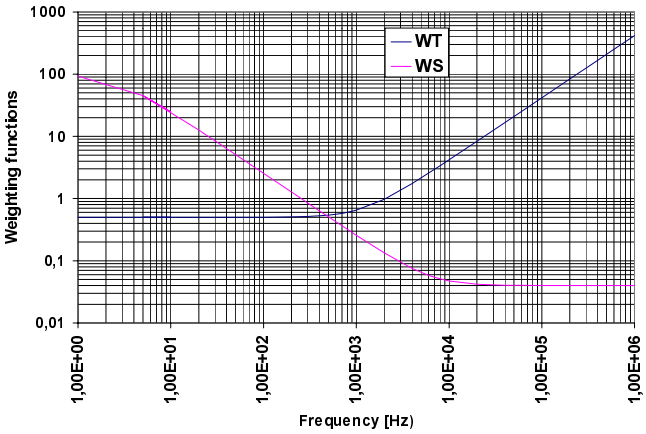

Fig. 5. Weighting functions.

In our case, the uncertainty weight chosen for the problem is:

$$W_{\mathrm{T}}(s) = \frac{s + 3000}{6000}\,. \tag{22}$$

The design of this particular transfer function is made according to the following observations:

- at low frequencies, there is potentially a 50% model variation;
- at the frequency ω_{T} (ω_{T} fixed at 5196 rad/s) the uncertainty in the model is up to 100% and may be larger at higher frequencies.

In this application, the performance weighting function is:

$$W_{\mathrm{S}}(s) = \frac{2s + 4 \times 10^4}{50s + 400}\,. \tag{23}$$

This function indicates that:

- at low frequencies, the closed-loop should reject disturbances at the output by a factor of 100-to-1. Thus, this function defines an attenuation factor on the noise on the output current which is provided by inverter harmonics and electromagnetic disturbances;
- the closed-loop system should perform better than open-loop for frequencies up to ω_{S} (ω_{S} fixed at 800 rad/s);
- for higher frequencies, closed-loop performance should degrade gracefully, but still lies underneath the inverse of W_{S}.

These weighting functions are represented Figure 5.

4.3 Controller design

Designing an H_∞ controller that achieves the conditions of performance and robust stability can be written as an

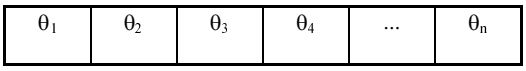

Fig. 6. Parameter representation.

optimization problem. The aim of this method is to find the parameters of the correctors which minimize

$$\left\| \begin{matrix} W_{\mathrm{S}} S \\ W_{\mathrm{T}} T \end{matrix} \right\|_{\infty}$$

below 1 [7–9,11].

H infinity synthesis needs several prerequisite conditions for the H infinity problem to be solvable [6,10]. But, even if the problem is solvable, we have to find the corrector by an optimization tool. Synthesis of H_∞ controllers is usually done using classical bisection or modified bisection methods. The iteration process is continued in an effort to approach the optimal H_∞ control design. The bisection methods search for the optimal solution between two high and low bounds and require tests to determine whether a solution exists for the H_∞ optimization problem.

Therefore, the algorithm convergence to the optimal solution is not guaranteed especially if the solution set presents suboptimal solutions. The order of the controller can be neither fixed nor modified using classical methods. This can convey to high order controllers depending on the order of the controlled plant and the weighting functions.

It is due to the optimization tool not to H infinity method. These disadvantages lead to the use of searching algorithms that would not converge to a suboptimal solution and find the optimal controller with a fixed structure of controllers. Thus, the genetic algorithm is used for the design of the current controllers.

Last	Objective	Copies number
string 1	5	1
string 2	9	2
string 3	2	1
string 4	2	1
string 5	0	0

Fig. 7. Reproduction example.

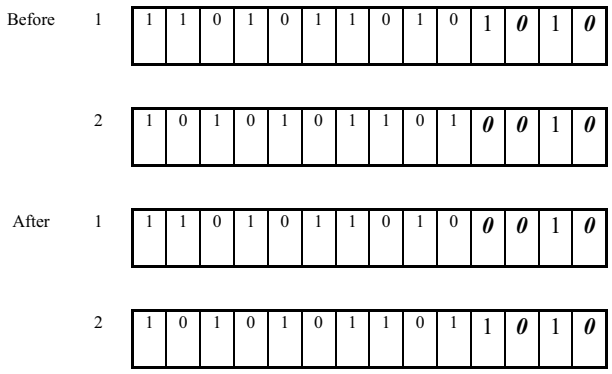

Fig. 8. Crossover example.

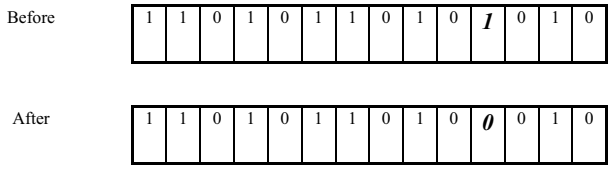

Fig. 9. Mutation example.

5 Genetic algorithm

Genetic algorithms are stochastic search tools based on life selection [13]. They are used to optimize multivariable function that may be discontinuous or not derivable.

It acts on a set of strings in which each parameter θ_i is concatenated after being coded (Fig. 6). An initial population of strings is arbitrarily created. Genetic algorithm makes it change by using three main operators (reproduction, crossover and mutation) in order to maximize an objective function.

Reproduction (Fig. 7) duplicates a string s_j according to the objective function value $f(s_j)$. Survival probability increases with higher value of $f(s_j)$. Let the objective function value associated with the jth individual denoted f_j, the sum of these values for the whole population f_{sum} and the mean value f_{mean}. Several criteria would be used to proceed reproduction using f_j/f_{sum} or f_j/f_{mean} ratio to determine the individuals that participate in the next generation. In our case, each individual is duplicated α times with $\alpha = \mathrm{ent}(f_i/f_{\mathrm{mean}})$. Population is completed by a maximum residual technique [13]. Reproduction can be preceded by a scaling of f in order to avoid undesirable convergence.

Then, for each pair of string, crossover is applied with a probability p_{cross}. If the crossover is decided, a place is chosen at random. All bits, from this location to the end, are swapped between the two strings. For instance, subset 1010 and 0010 are swapped in Figure 8.

Mutation is randomized alteration of each bit of each string with a certain probability p_{muta}. For instance, the bit number 3 (first one is bit number 0) is complemented in Figure 9.

The algorithm is represented Figure 10. Another criterion to stop the optimization process is to find a set of parameters such as the cost function becomes greater than a given number $1/\varepsilon$.

Main interest of genetic algorithm is not to provide high rate convergence but keep the possibility to test, at any time, a new set of parameters in the whole space of research. It avoids undesired convergence to a local optimum.

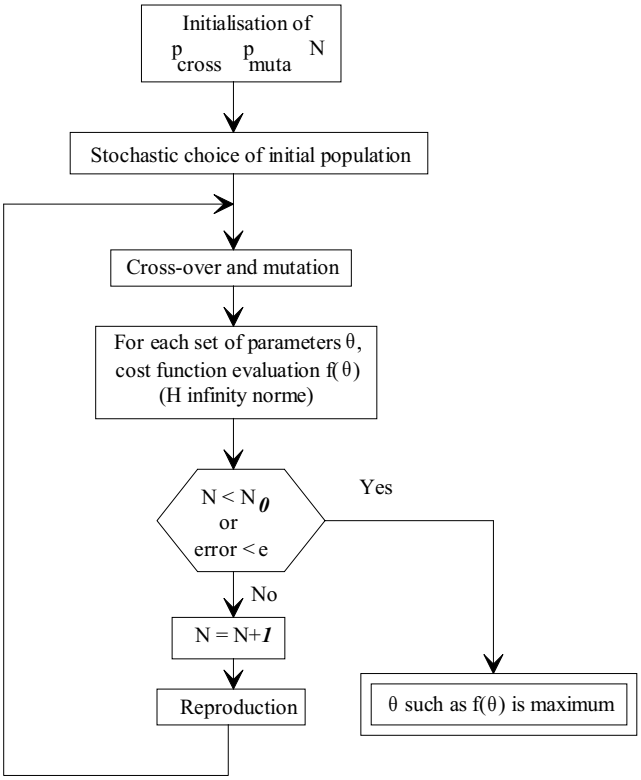

Fig. 10. Algorithm.

6 Application of genetic algorithm to H_∞ synthesis

The coefficients of the H_∞ controller are computed using the genetic algorithm described above in order to maximize

$$\frac{1}{\left\| \begin{matrix} W_\mathrm{S} S \\ W_\mathrm{T} T \end{matrix} \right\|_\infty} .$$

Genetic algorithms are used to optimize controllers which are designed with a given structure and a fixed order. These regulators must be proper and stable. All the poles are fixed in the left half plane. These considerations lead to the following controller structure:

$$H(s) = \frac{C(s)}{D(s)} = K \frac{c_1 s + c_0}{s^2 + \mathrm{d}_1 s + \mathrm{d}_0} \tag{24}$$

where c_0, d_0 and d_1 in $[0,\ 10^5]$, c_1 in $[0,\ 10^3]$ are the unknown parameters and $K = 10^3$. All the parameters of these controllers are 16 bits coded. Population was made of strings such as:

$$\theta = \begin{bmatrix} c_0 & c_1 & d_0 & d_1 \end{bmatrix} . \tag{25}$$

In order to fulfill additional constraints (closed loop stability, existence of the H_∞ norm ...), cost function is set to zero when these former conditions are not satisfied. Thus, reproduction eliminates unsuitable strings. Optimization

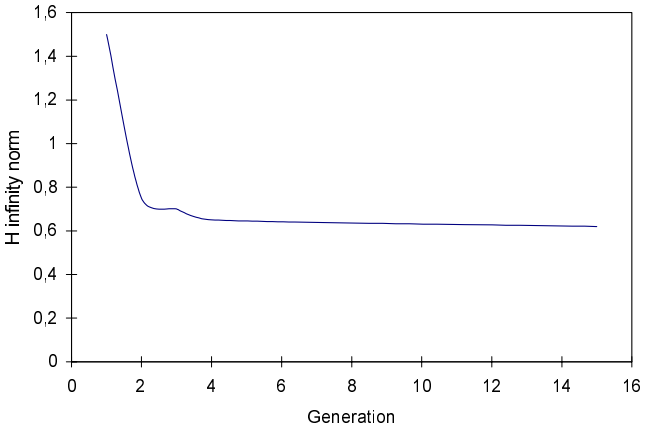

Fig. 11. Evolution of the infinity norm with the generations.

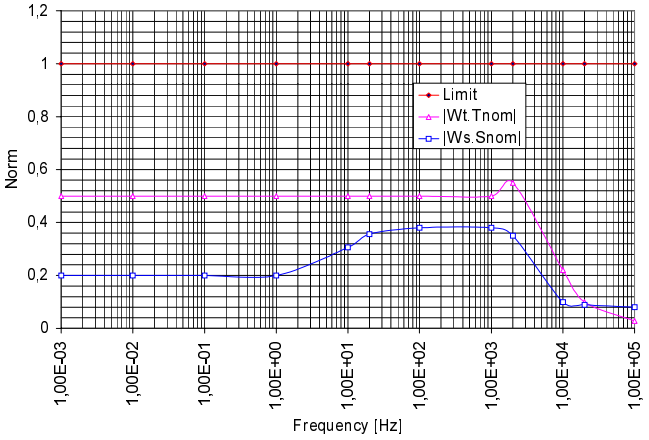

Fig. 12. Nominal performance and robust stability.

parameters are:

- $p_\mathrm{cross} = 0.66$;
- $p_\mathrm{muta} = 0.01$ (number of mutations must be low to keep a suitable rate of convergence);
- scaling factor = 0.5 (it provides compromise between deterministic and stochastic behaviour);
- population size = 30.

The synthesis is realized on the nominal system:

$$\begin{aligned} T_\mathrm{nom}(s) &= \frac{L_\mathrm{r} T_\mathrm{r}}{R_\mathrm{s} L_\mathrm{r} T_\mathrm{r} + L_\mathrm{m}^2 + \sigma L_\mathrm{s} L_\mathrm{r} T_\mathrm{r} s} \\ &= \frac{i_\mathrm{ds}}{\nu_\mathrm{ds11}} = \frac{i_\mathrm{qs}}{\nu_\mathrm{qs1}} . \end{aligned} \tag{26}$$

Figure 11 shows the evolution of the infinity norm during the optimization.

The synthesized controller

$$H(s) = 10^3 \, \frac{3.696 \times 10^2 s + 9.61 \times 10^4}{s^2 + 5353 s + 2.304 \times 10^4}$$

achieves nominal performance and robust stability of the nominal closed loop. Indeed, $\left\| W_\mathrm{S} S_\mathrm{nom} \right\|_\infty < 1$ and $\left\| W_\mathrm{T} T_\mathrm{nom} \right\|_\infty < 1$ (Fig. 12).

The s domain correctors are sampled with a w-transform in order to obtain the numeric equations.

7 Flux and rotor time constant estimation with reduced order extended Kalman filter

In an indirect field oriented scheme, current references and slip frequency are computed according to the following equations:

$$\omega_{\mathrm{sl}} = \frac{L_{\mathrm{m}}}{\phi_{\mathrm{r}}^{*} T_{\mathrm{r}}} i_{\mathrm{qs}}, \tag{27}$$

$$K_{\mathrm{d}} = \frac{i_{\mathrm{ds}}^{*}}{\phi_{\mathrm{r}}^{*}} = L_{\mathrm{m}}, \tag{28}$$

$$K_{\mathrm{p}} = \frac{i_{\mathrm{qs}}^{*}}{T_{\mathrm{e}}} = \frac{L_{\mathrm{r}}}{p L_{\mathrm{m}} \Phi_{\mathrm{dr}}}\,. \tag{29}$$

These references depend on rotor time constant and flux. Better accuracy can be obtained with on line estimation of these parameters. Thus, we have realized an extended reduced order Kalman filter [5,14–16].

Let us consider the state vector

$$X_1 = \begin{bmatrix} \Phi_{\mathrm{dr}} \\ \Phi_{\mathrm{qr}} \end{bmatrix} \quad \text{and} \quad U_1 = \begin{bmatrix} i_{\mathrm{ds}} \\ i_{\mathrm{qs}} \end{bmatrix}.$$

From (1), state space equation of rotor flux in synchronous reference frame can be written:

$$\frac{\mathrm{d}X_1}{\mathrm{d}t} = A_1 X_1 + B_1 U_1 \tag{30}$$

with $A_1 = \begin{bmatrix} -\sigma_{\mathrm{r}} & \omega_{\mathrm{sl}} \\ \omega_{\mathrm{sl}} & -\sigma_{\mathrm{r}} \end{bmatrix}$ and $B_1 = \begin{bmatrix} L_{\mathrm{m}}\sigma_{\mathrm{r}} & 0 \\ 0 & L_{\mathrm{m}}\sigma_{\mathrm{r}} \end{bmatrix}$.

Estimation requires sampling of this mathematical model:

$$X_1(k+1) = F(k+1,k) X_1(k) + H_1 U(k)$$

with

$$F(k,k+1) = \exp\left(\int_k^{k+1} A_1(\tau)\mathrm{d}\tau\right) \approx I + T_{\mathrm{ech}} A_1 + \frac{[T_{\mathrm{ech}} A]^2}{2}$$

and

$$H_1 = \int_k^{k+1} F(k,\tau) B \mathrm{d}\tau \approx T_{\mathrm{ech}} \left(I + \frac{A T_{\mathrm{ech}}}{2}\right) B.$$

In order to estimate the rotor time constant, the extended state vector

$$X_2 = \begin{bmatrix} \Phi_{\mathrm{dr}} \\ \Phi_{\mathrm{qr}} \\ \sigma_{\mathrm{r}} \end{bmatrix}$$

is introduced with $\sigma_{\mathrm{r}} = R_{\mathrm{r}}/L_{\mathrm{r}}$. σ_{r} is assumed to be constant during a sampling period:

$$\frac{\mathrm{d}\sigma_{\mathrm{r}}}{\mathrm{d}t} = 0 \quad \text{or} \quad \sigma_{\mathrm{r}}(k+1) = \sigma_{\mathrm{r}}(k) + \varepsilon_{\sigma_{\mathrm{r}}}(k)$$

with the error model $\varepsilon_{\sigma_{\mathrm{r}}}(k)$.

Thus, the numeric system can be written as:

$$X_2(k+1) = F_2 X_2(k) + H_2 U_2(k) \tag{31}$$

with

$$F_2 = \begin{bmatrix} 1 - T_{\mathrm{ech}}\sigma_{\mathrm{r}} + \frac{T_{\mathrm{ech}}^2}{2}(\sigma_{\mathrm{r}}^2 - \omega_{\mathrm{sl}}^2) & T_{\mathrm{ech}}\omega_{\mathrm{sl}} - T_{\mathrm{ech}}^2 \sigma_{\mathrm{r}}\omega_{\mathrm{sl}} & 0 \\ -(T_{\mathrm{ech}}\omega_{\mathrm{sl}} - T_{\mathrm{ech}}^2\sigma_{\mathrm{r}}\omega_{\mathrm{sl}}) & 1 - T_{\mathrm{ech}}\sigma_{\mathrm{r}} + \frac{T_{\mathrm{ech}}^2}{2}(\sigma_{\mathrm{r}}^2 - \omega_{\mathrm{sl}}^2) & 0 \\ 0 & 0 & 1 \end{bmatrix}$$

and

$$H_2 = \begin{bmatrix} 1 - \frac{\sigma_{\mathrm{r}} T_{\mathrm{ech}}}{2} & \frac{T_{\mathrm{ech}}^2 \omega_{\mathrm{sl}}}{2} \\ -\frac{T_{\mathrm{ech}}\omega_{\mathrm{sl}}}{2} & 1 - \frac{\sigma_{\mathrm{r}} T_{\mathrm{ech}}}{2} \\ 0 & 0 \end{bmatrix}.$$

These equations can be summarized with:

$$X(k+1)) = f(X(k),k) + \varepsilon$$

where ε designs the error model. Estimation process is governed by the following complex observation equation (delayed time Kalman filter):

$$\bar{z}_{\mathrm{dq}}^{\mathrm{m}}(k+1) = \bar{\Phi}_{\mathrm{r_{dq}}}(K+1) - \bar{\Phi}_{\mathrm{r_{dq}}}(k) + \bar{\lambda}_{\mathrm{dq}}(n+1) \tag{32}$$

with $\bar{\lambda}_{\mathrm{dq}}$ the measured error and $\bar{z}_{\mathrm{dq}} = z_{\mathrm{d}} + \mathrm{j} z_{\mathrm{q}}$.

Equation (32) can be rewritten as:

$$Z^{\mathrm{m}}(k+1) = LX(k+1) + JX(k) + \lambda(k) \tag{33}$$

with

$$Z^{\mathrm{m}} = \begin{bmatrix} Z^{\mathrm{m}}d \\ Z^{\mathrm{m}}q \end{bmatrix}, \quad H = \begin{bmatrix} 1\ 0\ 0 \\ 0\ 1\ 0 \end{bmatrix}$$

and

$$j = \begin{bmatrix} -1 & -T_{\mathrm{e}}\omega_{\mathrm{s}}(k)\ 0 \\ T_{\mathrm{e}}\omega_{\mathrm{s}}(k) & -1 \quad 0 \end{bmatrix}.$$

$\bar{z}_{\mathrm{dq}}^{\mathrm{m}}(k+1)$ can be evaluated from measures at sample kT_{e}:

$$z_{\mathrm{d}}^{\mathrm{m}}(k+1) = \frac{T_{\mathrm{e}} L_{\mathrm{r}}}{L_{\mathrm{m}}}[v_{\mathrm{ds}}(k) - R_{\mathrm{s}} i_{\mathrm{ds}}(k)] - \frac{\sigma L_{\mathrm{r}} L_{\mathrm{s}}}{L_{\mathrm{m}}}[i_{\mathrm{ds}}(k+1) - i_{\mathrm{ds}}(k) - T_{\mathrm{e}}\omega_{\mathrm{s}}(k) i_{\mathrm{qs}}(k)], \tag{34}$$

$$z_{\mathrm{q}}^{\mathrm{m}}(k+1) = \frac{T_{\mathrm{e}} L_{\mathrm{r}}}{L_{\mathrm{m}}}[v_{\mathrm{qs}}(k) - R_{\mathrm{s}} i_{\mathrm{qs}}(k)] - \frac{\sigma L_{\mathrm{r}} L_{\mathrm{s}}}{L_{\mathrm{m}}}[i_{\mathrm{qs}}(k+1) - i_{\mathrm{qs}}(k) + T_{\mathrm{e}}\omega_{\mathrm{s}}(k) i_{\mathrm{ds}}(k)]. \tag{35}$$

Thus predicted extended state $\tilde{X}(k+1) = f(\hat{X}(k),k)$ is corrected by measurements in order to provide the estimated extended state at $k+1$:

$$\hat{X}(k+1) = \tilde{X}(k) + G(k+1)\Big[z^{\mathrm{m}}(k+1) - H(\tilde{X}(k+1) + J\hat{X}(k))\Big] \tag{36}$$

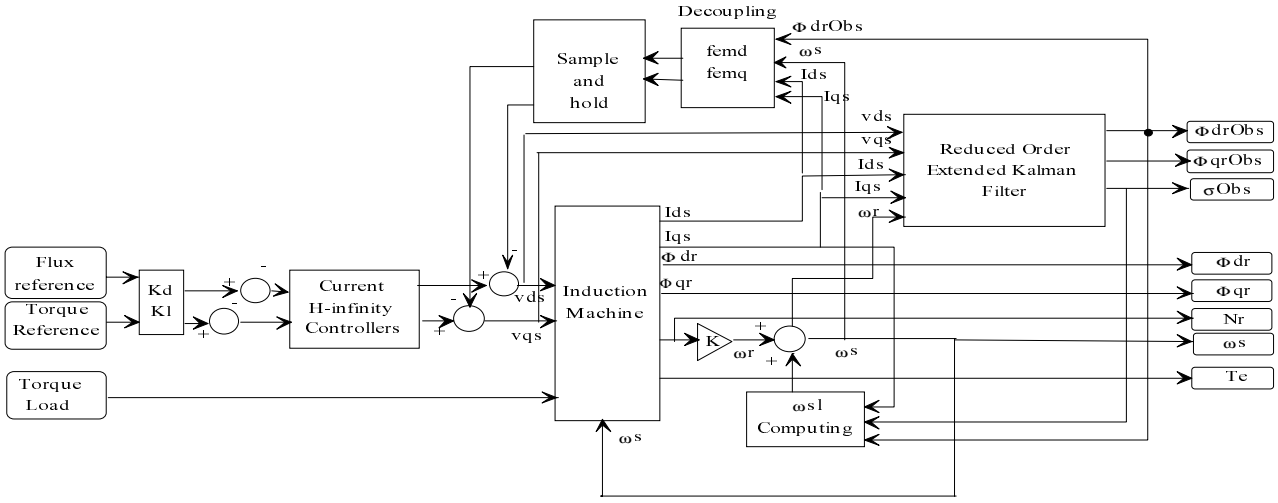

Fig. 13. System configuration with KALMAN filter and current regulators.

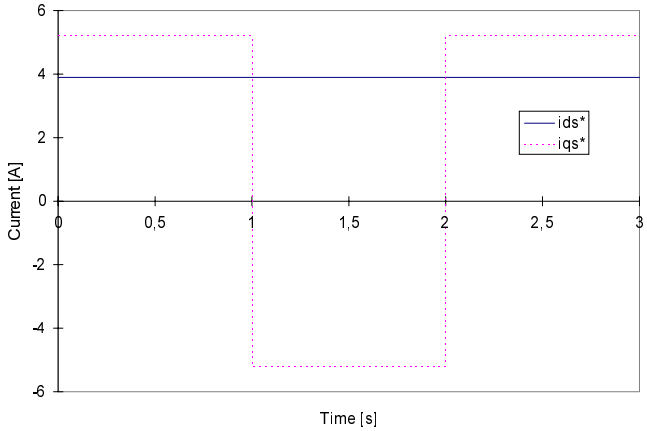

Fig. 14. Reference currents i_{ds}^{*} and i_{qs}^{*}.

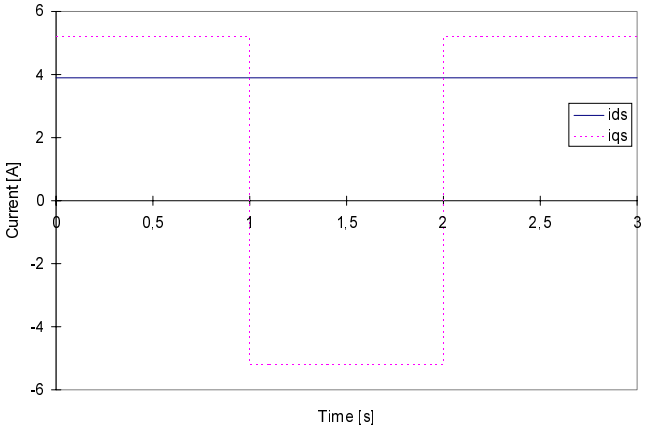

Fig. 15. Simulated currents i_{ds} and i_{qs} with nominal rotor resistance R_{r}.

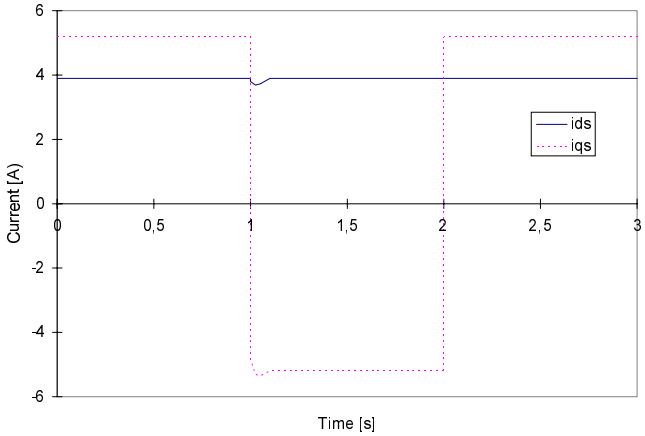

Fig. 16. Simulated currents i_{ds} and i_{qs} with 50% variation of rotor resistance R_{r}.

where G is the optimal gain matrix of the Kalman filter.

λ and ε are assumed to be uncorrelated random noise vectors with zero mean and covariance N and Q. The latter are defined empirically. According to Kalman filter theory [14], the estimator algorithm can be written as:

$$G(k+1) = (\tilde{P}(k+1)H^{\mathrm{T}} + \Phi(k)\hat{P}(k)J^{\mathrm{T}}) \times [H\tilde{P}(k+1)H^{\mathrm{T}} + N + J\hat{P}(k)J^{\mathrm{T}} + H\Phi(k)\hat{P}(k)J^{\mathrm{T}} + J\hat{P}(k)\Phi^{\mathrm{T}}(k)H^{T}]^{-1}$$

where

$$\tilde{P}(k+1) = \Phi(k)\hat{P}(k)\Phi^{\mathrm{T}}(k) + Q$$

$$\text{and} \quad [\Phi_{ij}] = \left[\frac{\partial f_i(X(k),k)}{x_j(k)}\right]_{X(k)=\hat{X}(k)}.$$

The whole process is represented in Figure 13.

8 Simulation and experimental results

The whole drive has been simulated on Simulink from Mathworks. The initial rotor resistance $R_{\mathrm{r_{drive}}}$ used to realize vector control orientation is taken equal to 50% of the nominal rotor resistance $R_{\mathrm{r_{motor}}}$ used to simulate the motor so as to validate rotor resistance tracking and flux estimation. The currents i_{ds}^{*} and i_{qs}^{*} references are fixed as shown in Figure 14.

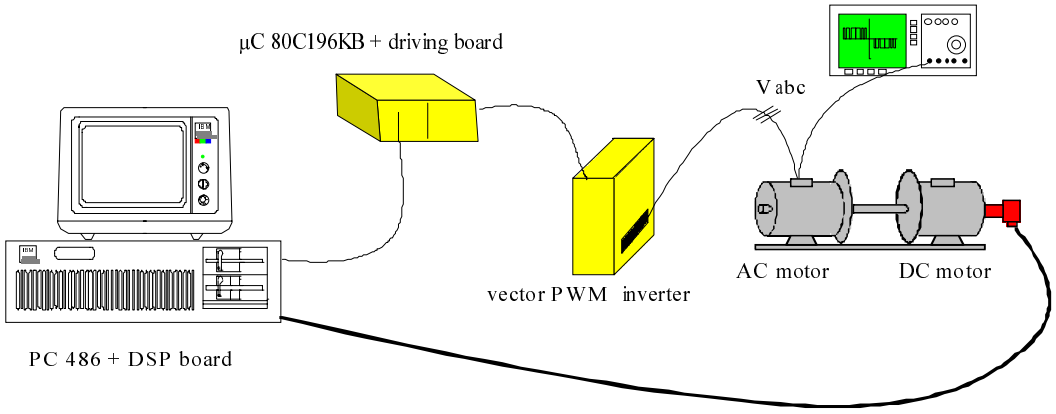

Fig. 17. Testing bench.

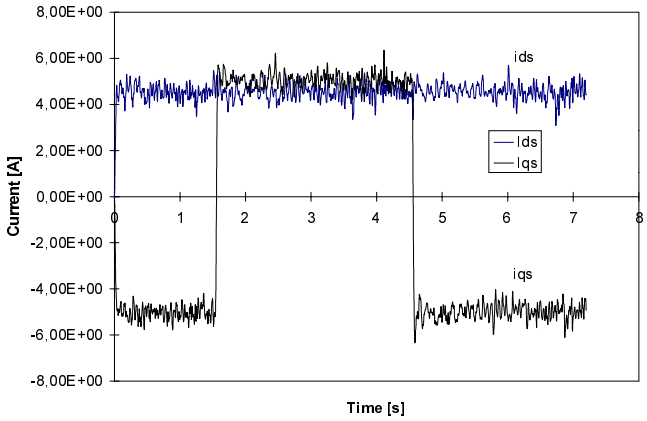

Fig. 18. i_{ds} and i_{qs} measured wave-forms.

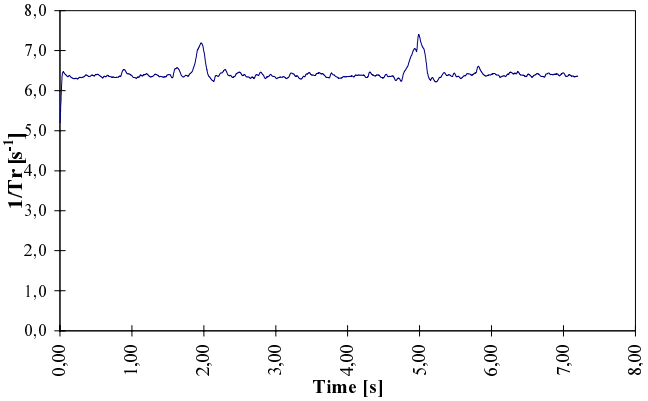

Fig. 19. Estimated inverse rotor time constant.

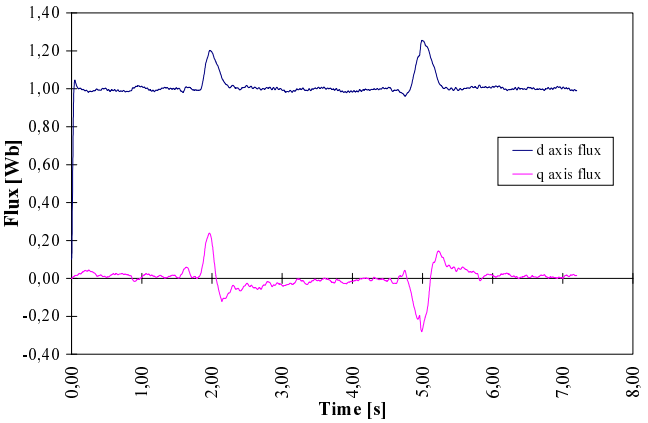

Fig. 20. Estimated rotor flux.

The synthesis of H_∞ controller with genetic algorithm led to the controller $H(s)$. This controller is placed in the current loops i_{ds} and i_{qs} in order to realize the regulation of the flux and torque currents respectively.

Figure 15 shows the torque and flux currents i_{qs} and i_{ds} in the case of nominal rotor resistance.

To be effective, the effects of model variation on the currents responses are evaluated with a simulation model including the eventuality of axes recoupling and loss of linearity. Model variation is simulated by a rotor resistance modification (Fig. 16).

In the case of rotor resistance variation, one can see perturbations on the flux orientation when the current i_{qs} varies in order to generate the required torque. This shows a brief interaction between torque and flux at that time.

However, these perturbations on the current i_{ds} are negligible and i_{qs} response remains acceptable.

These waveforms show that performances and stability are actually performed by these stable correctors. These low order regulators can be implanted on low cost micro-controller or digital signal processors.

On the contrary, usual H_∞ synthesis provides high order controllers which need powerful digital signal processors.

This method has been tested in a 220 V/380 V 5 kW induction machine bench (Fig. 17). PWM is implemented in a 80C196KB micro controller. A TMS320C31 DSP (DS1002 board from DSPACE) realized the current correctors.

The torque of the induction machine has been fixed to the square reference ± 15 Nm. This provides the behaviour of the induction machine near its nominal operating point with large scale sliding frequency step. Thus

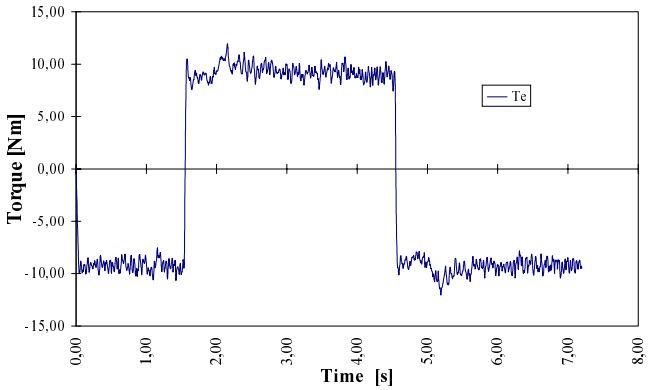

Fig. 21. Measured torque.

the rotor resistance and the speed vary (including reverse speed operation and generating mode).

Current waveforms has been registered (Fig. 18). The experimental waves are quite similar to the simulated ones. The current ripple is mainly due to measure and discretization.

The extended reduced order Kalman filter has been implemented in the same motor bench. The Figures 19–21 represent the estimated rotor d and q axis flux, the estimated inverse rotor time constant and the measured torque. The torque of the induction machine is still fixed to a square reference $\pm$ 15 Nm. Field orientation is maintained in spite of torque variation. Some perturbations appear since observers are not integrated in the H infinity synthesis but they are quickly cancelled (less than 500 ms). All those results shows the robustness of the algorithms and validate the method.

9 Conclusion

In this paper, we have presented a robust field oriented vector control of AC machine.

Inner currents loops are synthesized by H infinity method. Parameter optimization is done by genetic algorithm. It provides fixed second order and minimum phase controllers which are suitable for embedded applications. This new method fits the performance and robustness objectives with simple correctors.

Outer field and torque controls are adapted by a reduced order extended Kalman filter, which estimates the rotor flux and time constant in real time. Estimation is directly done in the synchronous frame in order to decrease CPU time.

Accuracy of the control has been proved by simulation and experimental results.

Further work will take into account the observers in order to decrease the flux disturbances We will consider the structure of the uncertainties in order to discriminate the influence of the rotor resistance and the magnetizing inductance and we will integrate the delays in the nominal transfer function for increasing control accuracy.

References

1. W. Leonhard, *Control of electrical drives* (Springer-Verlag, Germany, 1990).
2. B.K. Bose, *Power electronics and AC Drives* (New York, USA, Prentice-Hall, 1986).
3. M. Pietrzak-David, Ph.D. thesis, INP Toulouse, France, 1988.
4. Y. Fu, Ph.D. thesis, University of Montpelier, France, 1991.
5. D.R. Chouiter, G. Clerc, J.M. Retif, Ph. Auriol, H_∞ controllers design for field oriented asynchronous machines, in *Proceedings of the EPE Chapter Symposium*, Lausanne, Switzerland, October 1994.
6. J.C. Doyle, B.A. Francis, A.R. Tannenbaum, *Feedback control theory* (Macmillan Publishing Company, New York, 1992).
7. H. Kwakernaak, Automatica **29**, 255 (1993).
8. K. Glover, J.C. Doyle, Syst. Contr. Lett. **11**, 167 (1988).
9. J.C. Doyle, K. Glover, P. Khargonekar, B. Francis, IEEE Trans. Aut. Control. **34**, 831 (1989).
10. J.C. Doyle, K. Glover, P. Khargonekar, B. Francis, IEEE Trans. Indust. Electro. **45**, 488 (1998).
11. J.P. Friang, Ph.D. thesis, University of Paris XI, Orsay, France, 1996.
12. A. Ghazel, B. De Fornel, J.C. Hapiot, J. Phys. III France **6**, 943 (1996).
13. D.E. Goldberg, *Genetic algorithm in search, optimization and machine learning* (Addison Wesley, 1989).
14. R.G. Brown, P.Y.C. Hwang, *Introduction to random signals and applied Kalman filtering*, 2nd edn. (John Wiley and Sons, New York, 1992).
15. Salvatore, S. Stasi, L. Tarchioni, IEEE Trans. Industr. Electr. **40**, 496 (1993).
16. G.J. Armstrong, D.J. Atkinson, *A comparison of Model Reference Adaptive system and extended kalman filter estimators* (EPE Trondheim, Norway, 1997), pp. 1430–1433.